Analyst

PAPER

View Article Online
View Journal | View Issue

Cite this: *Analyst*, 2024, **149**, 4351

Corrective protocol to predict interference free sensor response for paper-based solution sampling coupled with heavy metal sensitive ion-selective electrodes†

Mingpeng Yang, [a,b,d] Rochelle Silva, [b,c,e] Ke Zhao, [b,c] Ruiyu Ding, [b] Jit Loong Cyrus Foo, [b] Liya Ge [b] and Grzegorz Lisak *[b,c]

Paper-based microfluidics combined with potentiometric measurement has emerged as an attractive approach for detecting various chemical ionic moieties. Detection of heavy metal ions, using paper substrates as solution sampling and delivery systems remains challenging despite efforts to introduce several physico-chemical paper substrate modifications to stop adsorption of ions onto the paper substrates. This study quantitatively investigates the adsorption of heavy metal ions on the paper substrates during paper-based potentiometric measurements and explains the super-Nernstian response of potentiometric sensors through local depletion of heavy metal ions from the solution. Consequently, based on the investigated ion adsorption, a corrective potential protocol was established for the electrodes coupled with paper-based solution sampling by predicting interference free sensor response from paper-based measurement. Furthermore, the ion adsorption was also recorded for mixed metal ion solutions to understand competitive primary/interfering ions adsorption onto the paper substrates and establish corrective measures to predict interference free sensor response. In this method, no modifications of the paper substrates are necessary before actual potentiometric measurements. The proposed corrective protocol allows prediction of sensor response based on the paper-based solution sampling potentiometric measurement, providing a simple methodological approach based on correction of potential readout of the potentiometric sensor, thus completely resigning from the need of modifying paper substrate for measurements of heavy metal ions.

Received 13th June 2024,
Accepted 5th July 2024

DOI: 10.1039/d4an00841c

rsc.li/analyst

1 Introduction

Heavy metal ions are considered common pollutants known for having long retention time in the environment, high toxicity, and the ability to accumulate in living organisms through the food chain.[1–3] Therefore, the reliable detection of heavy metal ions is crucial for preventing their detrimental impact on the environment and human health.[4–7] Potentiometric sensors offer an attractive and cost-effective approach for detecting heavy metal ions in aqueous samples due to their low power consumption, relatively short analysis time, and small sample volume requirement.[8–10]

In recent years, the potentiometric sensors combined with microfluidic technology have facilitated advanced sampling arrangements through applying various methods related to introduction of samples to the detection zone.[11–13] This has led to new applications, including environmental monitoring, management, and support of soil nutrients in agriculture, and medical diagnostics.[12,14–16] Paper-based microfluidics, utilizing paper substrates as the matrices for solution sampling, offers unique advantages to the applicability and cost of the potentiometric analytical devices, namely reducing sample consumption and filtering solid impurities, thus prolonging the life of the sensor and opening new possibilities for direct measurements in samples containing high solid to liquid ratios.[17–21]

[a]*School of Automation, Nanjing University of Information Science and Technology, 219 Ningliu Road, Nanjing 210044, China*
[b]*Residues and Resource Reclamation Centre, Nanyang Environment and Water Research Institute, Nanyang Technological University, 1 Cleantech Loop, CleanTech One, 637141 Singapore, Singapore. E-mail: g.lisak@ntu.edu.sg*
[c]*School of Civil and Environmental Engineering, Nanyang Technological University, 50 Nanyang Avenue, 639798 Singapore, Singapore*
[d]*Jiangsu Collaborative Innovation Centre on Atmospheric Environment and Equipment Technology, Nanjing University of Information Science and Technology, 219 Ningliu Road, Nanjing 210044, China*
[e]*Interdisciplinary Graduate Programme, Nanyang Technological University, 61 Nanyang Drive, Academic Block North, Singapore 637335, Singapore*
† Electronic supplementary information (ESI) available. See DOI: https://doi.org/10.1039/d4an00841c

On the other hand, the introduction of a paper substrate for solution sampling coupled with potentiometric sensors can promote parasitic processes of adsorption of ions onto the paper matrix, easily altering sample concentration, particularly when the volume is minimal. This is especially valid in heavy metal ions detection, as negatively charged sites, such as hydroxy and carboxyl groups in the paper substrates, attract positively charged heavy metal ions. The stronger the interaction between heavy metal ions with the paper substrates, the higher the local depletion of heavy metal ions at the detection zone. When paper-based microfluidic solution sampling is coupled with potentiometric sensors, depletion of heavy metals at the detection zone leads to super-Nernstian responses of ion-selective electrodes (ISEs) during calibration and ion detection. This phenomenon is mostly associated with the detection of heavy metals and has been studied extensively.[22,23] To overcome the super-Nernstian response of ISEs when coupled with paper-based microfluidic solution sampling, different strategies have been employed, including the use of inorganic salt-modified,[22] acidified,[23] metal-modified,[21] and ion-selective membrane-modified[20] paper substrates. These approaches aimed to reduce or avoid the adsorption of heavy metal ions during paper-based microfluidic solution sampling and improve the accuracy of paper-based potentiometric ion-selective electrodes (ISEs). Specifically, negatively charged sites in the hydroxy and carboxyl groups of the paper substrate are blocked by competitive ions or coatings, thereby suppressing the super-Nernstian response of the ISEs coupled with paper-based microfluidic solution sampling. Through the aforementioned approaches, approximately linear calibration curves of ISEs were obtained, enabling the detection of heavy metal ions within a defined linear range. However, these methods necessitate special treatment of the paper substrates, which may alter its inherent properties, such as diminishing the capillary effect of the paper or introducing complexity in paper substrate pre-treatment and handling. Additionally, in certain cases, the introduction of extraneous ions can increase interference and elevate the risk of environmental contamination of the sample.

Although several paper substrate modifications were proposed, the understanding of the Nernstian response of ISEs during heavy metal ion detection with paper-based microfluidic solution sampling coupled with potentiometric sensors, compared to direct solution-based methods, is still not fully understood. The calibration curves obtained by ISEs coupled with paper-based microfluidic solution sampling are dramatically different from those obtained in solution measurements. Although it is generally accepted that the adsorption of heavy metal ions onto the negatively charged sites of the paper substrate is the main contributing factor,[23] a precise understanding of the interactions of paper substrates with heavy metal ions across the entire concentration range is still lacking.

This paper presents a quantitative protocol to systematically investigate the effects of heavy metal ion adsorption onto the paper substrates during potentiometric measurements. The study focuses on understanding the influence of adsorption of heavy metal ions by paper substrates on the Nernstian response of ISEs, establishing the relationship between the adsorption of heavy metal ions and the Nernstian responses of potentiometric ISEs. Furthermore, the obtained quantitative data allowed for the high confidence prediction of the potential of potentiometric cell coupled with paper-based microfluidic solution sampling, purely based on measurements obtained from traditional solution-based approach and ion-paper substrate adsorption earlier determined. This opens new possibilities in direct measurements of heavy metal ion concentrations without applying modifications to the paper substrates.

2 Experimental

2.1 Chemicals, materials, and electrodes

Lead nitrate ($Pb(NO_3)_2$), cadmium nitrate ($Cd(NO_3)_2$), 70% nitric acid (HNO_3), poly(sodium-*p*-styrenesulfonate) (NaPSS), 3,4-ethylenedioxythiophene (EDOT), lead ionophore IV, cadmium ionophore I, potassium tetrakis(4-chlorophenyl) borate (KTClPB), 2-nitrophenyl octylether (o-NPOE), poly(vinyl chloride) (PVC), and tetrahydrofuran (THF) were procured from Sigma-Aldrich (Germany) with a purity of ≥99%. Sartorius filter paper (no. 389, particle retention 8–12 μm) was used, and the InLab® Surface Pro ISM pH electrode (flat glass membrane electrode) was coupled with the Seven Compact pH/ion S220 meter from Mettler-Toledo (Switzerland). The reference electrode was a single junction silver/silver chloride (in 3 M KCl) electrode from Thermo Fisher (USA), and the glassy carbon (GC) disk electrodes (3 mm) were purchased from X2 Lab Pte. Ltd (Singapore). Ultra-pure water (18 MΩ cm) from the Milli-Q Integral Water Purification System (USA) was used to prepare all aqueous solutions.

Initially, GC electrodes were polished using 0.3 μm alumina (Al_2O_3) slurry on a soft pad, and subsequently rinsed with ultra-pure water. The electropolymerization of PEDOT:PSS on GC electrodes was performed using a three-electrode cell consisting of a working electrode (GC electrode), a counter electrode (Pt mesh electrode), and a reference electrode (Ag/AgCl electrode). A constant current of 0.014 mA (0.2 mA cm^{-2}) was applied for 714 s in a prepared electropolymerization solution comprising 0.1 mol L^{-1} NaPSS and 0.01 mol L^{-1} EDOT,[24] followed by rinsing with ultra-pure water and drying in the open air at room temperature (23 ± 2 °C) for 12 hours. To prepare the Pb^{2+} selective membrane, a membrane cocktail (100 mg solutes containing 1 wt% lead ionophore (IV), 0.5 wt% KTClPB, 33.3 wt% PVC, and 65.2 wt% o-NPOE dissolved in 2 mL THF) was dropped onto the electrode for three times with a volume of 20 μL for each droplet and with an interval of one hour between droplets. The electrodes were then dried in open air at room temperature (23 ± 2 °C) for 12 hours. Before testing, the electrodes were conditioned in 10^{-3} mol L^{-1} $Pb(NO_3)_2$ for 12 hours. Similar procedures were followed to prepare the Cd^{2+}-ISEs. The Cd^{2+}-ISEs were prepared in the same way but using a membrane cocktail of 100 mg solutes containing 1 wt% cadmium ionophore, 1.02 wt% NaTFPB, 32.66 wt% PVC, and 65.32 wt% o-NPOE.

2.2 Potential measurements with Pb^{2+}- and Cd^{2+}-ISEs in conventional beaker-based and with paper-based microfluidic solution sampling

Before commencing potentiometric measurements, the Pb^{2+}- and Cd^{2+}-ISEs were conditioned for 12 h in 10^{-3} mol L^{-1} Pb$(NO_3)_2$ and Cd$(NO_3)_2$ solutions, respectively. To perform potentiometric measurements utilizing paper-based microfluidic sampling in conjunction with Pb^{2+}- and Cd^{2+}-ISEs, filter paper (no. 391, particle retention, 2–3 μm) was cut into small pieces (15 mm × 15 mm). The cut paper pieces were meticulously washed with ultra-pure water to ensure removal of any water-soluble components from the paper. Subsequently, the washed paper was oven-dried at 60 °C for one hour and allowed to dry at room temperature.

The potentiometric measurements were conducted with an EMF 16 potentiometer (Lawson Labs). The potentiometric response of each measurement was recorded for 60 s at room temperature (23 ± 2 °C). Standard Pb$(NO_3)_2$ and Cd$(NO_3)_2$ solutions from 10^{-7} to 10^{-1} mol L^{-1} were used in the sequence of increasing ion concentrations. Standard deviation was determined by conducting three consecutive measurements of the same sample type (n = 3).

In this study, the potentiometric measurements were initially conducted directly in a beaker using the prepared Pb^{2+}- and Cd^{2+}-ISEs. Subsequently, the calibrated ISEs with known Nernstian responses in beaker-based measurements were employed to perform potentiometric measurements with the assistance of paper-based microfluidic sampling. For each test, 90 μL of the sample was pipetted onto the prepared paper substrate first. The ISE and a single-junction Ag/AgCl (3 M KCl) reference electrode were then fixed side by side and erected on the paper substrate sheet. Continuous potential data of the potentiometric cell was recorded for 60 s, and the paper substrate was changed to a new one for each subsequent measurement.

2.3 Protocol for determining adsorption of heavy metal ions onto the paper substrates

Before the use, all paper substrates were thoroughly washed with ultra-pure water and subsequently dried in an oven at 60 °C for 1 hour and dried at room temperature. Based on the liquid wicking capacity of the no. 389 filter paper,[22] a 90 μL aqueous sample was required for a single detection using a 15 mm × 15 mm paper substrate (Fig. 1(a)). However, the amount of sample remaining after adsorption on the paper substrate was insufficient for ICP-OES analysis. To overcome this issue, the sample amount was increased by 20-fold, as illustrated in Fig. 1(b), by immersing 20 pieces of paper with a size of 15 mm × 15 mm in 1.8 mL of the samples (solutions with single or mixed ions) for 1 minute. Subsequently, 0.5 mL of the remaining solutions were pipetted and subjected to ICP-OES analysis to determine the concentration of the heavy metal ions remaining in the solution indicating the adsorption of heavy metals from respective solutions.

In this study, adsorption is quantitatively defined as the ability of paper substrates to absorb metal ions from a solution. Specifically, it denotes the ratio of the amount of ions absorbed by the paper substrates to the total amount of ions present in the solution prior to any interaction between the substrate and the solution. Additionally, the volume of the solution assessed here is the capacity that the paper substrate can accommodate. The adsorption of Pb^{2+} and Cd^{2+} onto the paper substrates was specifically measured within a concentration range spanning from 10^{-5} to 10^{-1} mol L^{-1}. Real environmental samples often contain a mixture of various heavy metal ions, making the analysis more complex. For example, the presence of interfering ions can occupy the binding sites on the paper substrate, leading to competition with the primary ion, thus impacting the adsorption of the primary ion. Consequently, the adsorption of heavy metal ions under complex conditions (mixed solutions) on the paper substrate was determined using the same method.

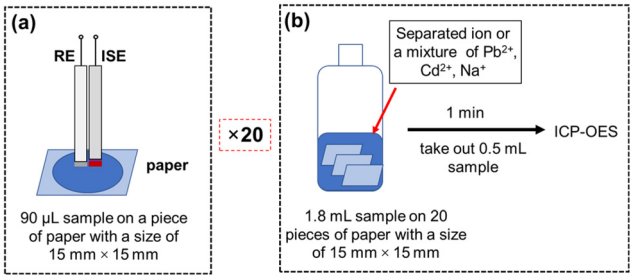

Fig. 1 (a) Conventional paper-based microfluidic solution sampling coupled with potentiometric cell; (b) protocol for determining the adsorption of heavy metal ions onto the paper substrates.

The above-mentioned measurements can provide information about the adsorption of heavy metals only at selected concentrations of Pb^{2+} or Cd^{2+}, creating discrete data points within the entire concentration range. In practical analyses, the concentrations of heavy metal ions in real samples can vary, and may not be aligned with these specific concentrations. If accurate information about the amount of heavy metal ion(s) of real samples adsorbed by the paper substrate is needed, it is necessary to know the adsorption of heavy metal ions onto the paper substrates at any concentration. To address this issue, this study employed a polynomial fitting method to approximate the adsorption of Pb^{2+} at any concentration, and the accuracy of the fitted results was experimentally verified.

2.4 Prediction of the potential of potentiometric cell coupled with paper-based microfluidic solution sampling derived from solution-based measurement

By knowing both the potential of the ISEs directly measured in the conventional solution-based measurement (the potential obtained by this method is further referred to as solution-based potential) and the adsorption of specific ions onto the paper substrates, the potential of the ISEs coupled with paper-based microfluidic solution sampling (the potential obtained by this method further referred to as paper-based potential)

can be predicted. The Nernst equation can be used to calculate the predicted potential of the ISE as follows:

$$E = E^{\circ} + S\log(a) \quad (1)$$

where E is the measured potential, E° is the standard potential, S is the response slope, and a is the ion activity.

Initially, the Nernstian responses of the prepared ISEs were recorded in standard solutions with concentrations spanning from 10^{-7} to 10^{-1} mol L^{-1}, and their calibration curves were obtained using the least-squares method. Within the linear function describing the calibration curves, the values of E° and S, which are inherently dependent on the properties of the ISEs, were determined. Subsequently, these Nernstian equations, equipped with known parameters, were employed to estimate the potential of potentiometric cell coupled with paper-based microfluidic solution sampling.

Supposing the adsorption of the heavy metal ions on the paper substrates at the concentration of c mol L^{-1} is r%, then $(100 - r)$% of the total heavy metal ion remains in the solution that was adsorbed onto the paper substrates. As such, the potential values of the ISEs in the presence of the remaining heavy metal ion can be calculated using the Nernst eqn (1) as:

$$E = E^{\circ} + S \times \log[(100 - r) \times 10^{-2} \times c \times \gamma] \quad (2)$$

where, γ represents the ion activity coefficient; c represents the concentration of ion in the sample before its contact with the paper substrate; and r signifies the adsorption of the ion on the paper substrate.

Once ISEs were directly tested in beaker-based measurements with standard solutions, their Nernstian responses coupled with paper-based microfluidic sampling were subsequently evaluated through empirical means. The data obtained from these experiments were utilized to evaluate the accuracy of the predicted potential readout of the ISEs.

2.5 Interference free electrode potential prediction from the measurement assisted with paper-based microfluidic solution sampling

The Nernstian responses of ISEs in standard solutions can also be predicted from the measurements of ISEs coupled with paper-based microfluidic solution sampling, provided that the adsorption of the heavy metal ions on paper substrates is previously understood. The prepared Pb^{2+}-ISEs coupled with paper-based microfluidic sampling were tested with standard $Pb(NO_3)_2$ solutions with concentrations from 10^{-7} mol L^{-1} to 10^{-1} mol L^{-1}. The potentials of Pb^{2+}-ISEs coupled with paper-based microfluidic sampling were recorded. Assuming that the potential of the Pb^{2+}-ISEs directly tested in the $Pb(NO_3)_2$ solution with a concentration of 10^{-i} mol L^{-1} is ${E_s}^{-i}$, according to the Nernst equation is:

$${E_s}^{-i} = E^{\circ} + S\log[\gamma_i \times 10^{-i}] \quad (3)$$

where, γ_i represents the ion activity coefficient when its concentration is 10^{-i}.

The potential of the Pb^{2+} ISEs coupled with paper-based microfluidic sampling in the $Pb(NO_3)_2$ solution with a concentration of 10^{-i} mol L^{-1} was measured, the value was ${E_p}^{-i}$, according to the Nernst equation is:

$${E_p}^{-i} = E^{\circ} + S\log[\gamma_i \times 10^{-i} \times (100 - r_i) \times 10^{-2}] \quad (4)$$

where, r_i is the adsorption of Pb^{2+} on the paper substrate when its concentration is 10^{-i} mol L^{-1}.

Similarly, assuming the potential of the Pb^{2+}-ISEs directly tested in the $Pb(NO_3)_2$ solution with a concentration of $10^{-(i+1)}$ mol L^{-1}, is:

$${E_s}^{-(i+1)} = E^{\circ} + S\log[\gamma_{(i+1)} \times 10^{-(i+1)}] \quad (5)$$

where, γ_{i+1} represents the ion activity coefficient of Pb^{2+} at a concentration of $10^{-(i+1)}$ mol L^{-1}.

In this study, these Pb^{2+}-ISEs coupling with paper-based microfluidic solution sampling were tested in the $Pb(NO_3)_2$ solution with a concentrations of $10^{-(i+1)}$ mol L^{-1}:

$${E_p}^{-(i+1)} = E^{\circ} + S\log[\gamma_{(i+1)} \times 10^{-(i+1)} \times (100 - r) \times 10^{-2}]. \quad (6)$$

By combining and solving eqn (3)–(6), we can obtain the value of ${E_s}^{-i}$ and ${E_s}^{-(i+1)}$.

Therefore, with this method, the potential values of Pb^{2+} tested in solutions can be predicted from those tested on the paper substrates.

2.6 Quantitative analysis of heavy metal ions in complex samples done by potentiometric cell coupled with paper-based microfluidic solution sampling

To address the possibility of influence of interfering ions on the potential formation of the potentiometric cell, six typical interfering ion pairs (cases) were identified (ESI, Table S1†). For Pb^{2+} determination, as indicated elsewhere,[22] it is important to note coupling Pb^{2+}-ISEs with paper-based solution sampling can be particularly challenging due to electrode super-Nernstian response as a result of the strong affiliation of Pb^{2+} to the paper matrix. This presents additional difficulties in achieving accurate measurements compared to other heavy metal ions such as Cd^{2+}. For this reason, we selected Pb^{2+} as the primary ion for these complex measurement cases and chose different interfering ions based on the selectivity reported for lead ionophore IV.[25–27]

In order to realize the analysis of Pb^{2+} in complex samples, two aspects of electrode response should be addressed, namely (i) selectivity of Pb^{2+}-ISEs, and (2) adsorption of Pb^{2+} on paper substrates in complex samples. To assess the selectivity of the Pb^{2+}-ISEs, it is necessary to investigate their responses to complex samples that may contain multiple types of ions (refer to Table S1†). Before conducting the selectivity tests, the Pb^{2+}-ISEs were conditioned in a solution of lead(II) nitrate with a concentration of 10^{-3} mol L^{-1} for a duration of 12 hours. For each case, three sets of tests were carried out using the following solutions: (i) solutions with the interfering ions (concentration ranging from 10^{-7} mol L^{-1} to 10^{-1} mol L^{-1}), (ii) solutions with the primary ions (concentration

ranging from 10^{-7} mol L^{-1} to 10^{-1} mol L^{-1}), and (iii) solutions with mixed ions (concentration of the primary ions ranging from 10^{-7} mol L^{-1} to 10^{-1} mol L^{-1}, while the concentration of interfering ions varied according to Table S1†). Each set of tests was performed at an interval of 1 hour to allow for the reconditioning of the Pb^{2+}-ISEs, thus eliminating the effect of previous measurements in solutions of different concentrations on subsequent measurements.

The presence of interfering ions in complex samples (Table S1†) may affect the adsorption of the primary ions on the paper substrates, and consequently influence the potential formation of the primary ions obtained by the ISEs. To assess this effect, the adsorption of Pb^{2+} on paper substrates in complex samples was investigated using the testing method described in Section 2.3. Additionally, the adsorption of the interfering ions on paper substrates was also investigated. Similar to the corrective procedure employed in case 1, in which no other interfering ions were present, a polynomial fitting method was used to approximate the adsorption of lead ions at any given concentration under the multiple scenarios, as listed in Table S1.† The accuracy of the fitting method was verified through experimental validation. Different from the detection of samples containing a single type of ions, the detection of complex samples requires consideration of selectivity of the ISE and the influence of interfering ions on the adsorption of the primary ion. For the selectivity, the well-conditioned Pb^{2+}-ISEs exhibiting excellent ion-selective performance were used. In most cases, the presence of interfering ions had only a minor influence on the potential response of the primary ions, as described in section 3.4. Therefore, when the adsorption of the primary ion (Pb^{2+}) on the paper substrates in complex samples was known, the solution-based potential could be calculated from the paper-based potential in complex samples using the method described in section 2.5.

2.7 Determination of Pb^{2+} in samples containing real background matrices

Lake water was collected from a rain collecting point (drain) linked to a lake in the Nanyang Technological University (NTU) campus, and primarily consisted of rainwater. Laboratory recycling water was obtained from tap water treated by the wastewater purification system, while laboratory wastewater was collected directly from an environmental laboratory at NTU. The composition of these background matrix solutions was determined using ICP-OES. To prepare lead-containing samples with real background electrolyte, a solution of Pb^{2+} with a concentration of 1 mol L^{-1} was prepared and a random volume between 0 and 1 mL was added to each of these background matrix solutions with a total volume of 5 mL.

Using the method described above, the approximate composition of interfering ions in the test solution could be determined in advance. This allowed for identification of specific case to which the sample belonged, as shown in Table S1.† In practical applications, the classification of a sample could be determined based on historical data or a small number of test samples. Once the sample is assigned to a specific case, the potential recovery method described in section 2.6 would be used to establish the calibration curve of the sensor. This calibration process could be carried out in advance and remain effective for a certain period of time.

$$E = E^{\circ} + S\log(a) \tag{7}$$

In eqn (8), E represents the measured potential, while E° denotes the standard potential value; S denotes the response slope; and a denotes the ion activity. The calibration curve equation involves the known values of E° and S, and allows for the determination of a by measuring E. The relationship between ion activity, a and concentration, c is described by the following expression:

$$a = \gamma c(100 - r) \times 10^{-2}. \tag{8}$$

In eqn (9), γ represents the ion activity coefficient; c represents the concentration of ion in the sample before it was in contact with the paper substrate; and r represents the adsorption of the ion on the filter paper, and can be represented by the fitting equation (Fig. S1–S6, ESI†).

The ion activity coefficient γ is dependent on the concentration of the solution, and can be calculated using the following two formulas[28–30]:

$$\gamma = -Az^2\frac{\sqrt{I}}{1 + Bs\sqrt{I}} \tag{9}$$

$$I = \frac{1}{2}\sum c_i z_i^2. \tag{10}$$

In eqn (9) and (10), I is ionic strength; $A = 1.82 \times 10^6(\varepsilon T)^{-2/3}$ (where ε is dielectric constant); $B = 50.3(\varepsilon T)^{-1/2}$; z is the charge of ion; s is an adjustable parameter (angstroms) corresponding to the size of the ion.[30] Finally, using eqn (7)–(10) described above, the concentration of ion in the sample can be calculated based on the measured potential value.

3 Results and discussion

3.1 Adsorption of Pb^{2+} and Cd^{2+} by paper substrates during paper-based microfluidic solution sampling

The adsorption of Pb^{2+} and Cd^{2+} by paper substrates was systematically investigated in pure samples containing a single ion concentration, and the results are shown in Fig. 2. Generally, with the increase of the concentrations of the heavy metal ions (Pb^{2+} and Cd^{2+}), their adsorption on paper substrate decreased. Compared with Cd^{2+}, the adsorption of Pb^{2+} was significantly higher when the concentrations ranged from 10^{-5} to 10^{-3} mol L^{-1}. Paper substrates possess abundant functional groups, such as carboxyl and hydroxyl, which can form coordination bonds with heavy metal ions. Compared to Cd^{2+}, Pb^{2+} exhibits a stronger polarizing ability, allowing them to form more stable coordination bonds with these functional groups. The larger ionic radius of Pb^{2+} enables it to bind with multiple coordination sites on the paper substrate, thereby enhancing its adsorption capacity through multi-site coordi-

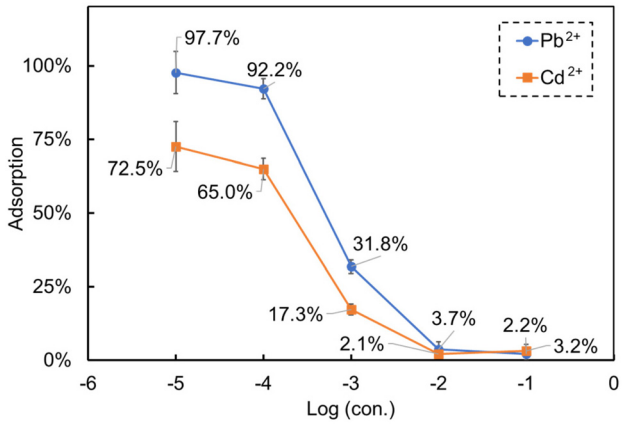

Fig. 2 Adsorption of Pb^{2+} and Cd^{2+} onto the paper substrates during paper-based potentiometric measurements in pure samples containing a single ion concentration.

nation. Consequently, these factors contribute to a higher adsorption capacity of Pb^{2+} on the paper substrate compared to Cd^{2+}. This conclusion is consistent with findings from previous studies.[31–33] However, when the concentrations range from 10^{-2} to 10^{-1} mol L^{-1}, the adsorption of the two ions became similar. Specifically, at the concentration of 10^{-5} mol L^{-1}, the adsorption of Pb^{2+} reached 97.7%, indicating that the concentration of remaining Pb^{2+} after adsorption was 2.3×10^{-7} mol L^{-1}. When the concentrations of the two heavy metal ions ranged from 10^{-2} mol L^{-1} to 10^{-1} mol L^{-1}, their adsorption reached the lowest value and varied negligibly. Thus, to summarize, the adsorption of the heavy metals onto the paper substrate is in a non-linear function with the concentration of the heavy metal ions in the solution. Paper substrates have limited capacity to accommodate heavy metal ions and thus the effect is most visible at low analyte concentrations, where nearly all ions are being taken up by the paper substrate. This poses practical challenges in terms of predicting the potential of ISEs when in contact with different ion concentrations.

3.2 Estimation of the potential of potentiometric cell coupled with paper-based microfluidic solution sampling derived from solution-based measurement

Using corrective methodology for the potential of ISEs described in section 2.4, the paper-based potential for the potentiometric measurements of Pb^{2+}-ISEs was predicted from the solution-based potential with the concentration-based adsorption of Pb^{2+} onto paper substrates (Fig. 3(a)). The predicted potential closely matched the measured potential obtained from paper-based potentiometric measurements with Pb^{2+}-ISEs, demonstrating the remarkable accuracy and effectiveness of the proposed prediction method. In the high concentration range (from 10^{-2} to 10^{-1} mol L^{-1}), the paper-based potential closely aligned with the solution-based potential. A previous study had shown that the adsorption amount of heavy metal ions on the paper substrate increases with their concentrations.[22] However, the adsorption percentage of heavy metal ions on paper substrate decreases with increasing concentrations of heavy metal ions, reaching a low level (less than 5%). As a result, the paper-based potential and the solution-based potential are closely matched. In the low concentration range (from 10^{-7} to 10^{-5} mol L^{-1}), the paper-based potential of Pb^{2+}-ISEs is nearly unresponsive (non-Nernstian), similar to what was observed elsewhere.[22,34] For the concentrations 10^{-7} to 10^{-6} mol L^{-1}, both the solution-based and paper-based potential showed minimal variations, due to the concentrations being below or close to the detection limit of the sensors. However, a difference was observed at a concentration of 10^{-5} mol L^{-1}, where the paper-based potential remained non-Nernstian while the solution-based potential exhibited close-to-Nernstian response. At this concentration, the adsorption of Pb^{2+} on the paper substrates exceeded 90%, resulting

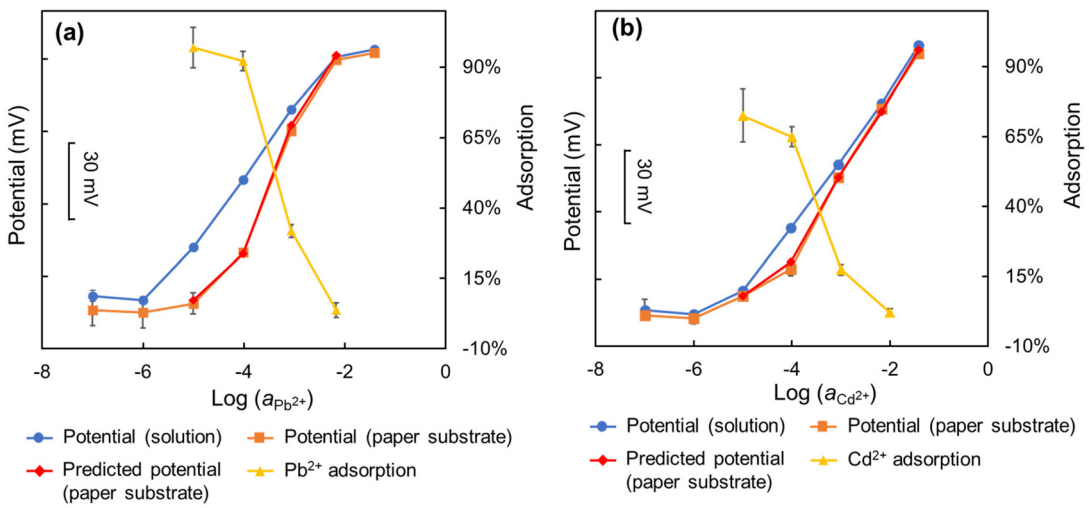

Fig. 3 Corrective protocol to predict interference free sensor response of ISE coupled with paper-based microfluidic solution sampling from solution-based measurement of (a) Pb^{2+}- and (b) Cd^{2+}-ISEs.

in the remaining Pb^{2+} concentration in the solution being less than 10% of 10^{-5} mol L^{-1} (10^{-6} mol L^{-1}). Consequently, the paper-based potential at the concentration of 10^{-5} mol L^{-1} for Pb^{2+} is close to that at a concentration of 10^{-6} mol L^{-1}. In the middle concentration range (from 10^{-4} to 10^{-3} mol L^{-1}), the solution-based potential continues to show a Nernstian response (approx. 29.2 mV dec^{-1} in Fig. 3(a)), whereas the paper-based potential suffers from super-Nernstian response (approx. 50.5 mV dec^{-1} in Fig. 3(a)). In both concentrations of 10^{-4} and 10^{-3} mol L^{-1}, the potential of Pb^{2+}-ISEs obtained on the paper substrates are lower than those obtained in the standard solutions due to the adsorption of heavy metal ions on the paper substrates. Furthermore, for paper-based measurements, the adsorption of Pb^{2+} on the paper substrates at the concentration of 10^{-4} mol L^{-1} is much higher than that at the concentration of 10^{-3} mol L^{-1}, resulting in a greater decrease in the potential (compared with the solution-based potential) at the concentration of 10^{-4} mol L^{-1} than that at the concentration of 10^{-3} mol L^{-1}. Consequently, the results obtained using the paper-based potentiometric method exhibit super-Nernstian response in this concentration range.

Similar results were observed in the measurement with Cd^{2+}-ISEs using the paper-based potentiometric method (Fig. 3(b)).

The remarkable recovery of the potential of the electrode based solely on adsorption, suggests that the mechanism driving the super-Nernstian response of ISEs is mostly dependent on the adsorption related phenomena between the ions and the paper substrate. This, however, does not answer what is the type of interactions within the adsorption (physical, chemical, or both). Also, the paper-based potentiometric measurement with Pb^{2+}-ISEs exhibits a more pronounced super-Nernstian response compared to that of Cd^{2+}-ISEs. This indicates that the detection of Pb^{2+} is more challenging using paper-based potentiometric methods than Cd^{2+}. Therefore, the subsequent studies focus solely on the measurements of Pb^{2+}.

3.3 Corrective electrode potential prediction in a conventional solution-based potential readout from the measurement assisted with paper-based microfluidic solution sampling

It was investigated that the conventional solution-based potential of the electrode can also be recovered from the measurement assisted with paper-based microfluidic solution sampling using the method described in section 2.5. In this instance, however, there is a limitation on the concentration range of the recovered potential readout. For example, for the concentration of 10^{-6} mol L^{-1} the concentration of remaining Pb^{2+} after adsorption onto the paper substrates is below the detection limit of the fabricated Pb^{2+}-ISEs (10^{-7} mol L^{-1}). Consequently, the valid calculation range for the paper-based potential of Pb^{2+} ISEs is from 10^{-5} mol L^{-1} to 10^{-2} mol L^{-1}. As shown in Fig. 4(a), the conventional solution-based potential (ranging from 10^{-5} mol L^{-1} to 10^{-2} mol L^{-1}) of Pb^{2+}-ISE was successfully recovered from the measurement assisted with paper-based microfluidic solution sampling accounting for the adsorption of Pb^{2+} onto the paper substrates at different concentrations. It was found that the conventional solution-based and corrected protocol-based measurements have very good agreement in terms of the potential readouts and slopes (Fig. 4(b)), demonstrating the effectiveness of the proposed corrective protocol method. This indicates, that by recovering the conventional solution-based potential of the electrode from the measurement assisted with paper-based microfluidic

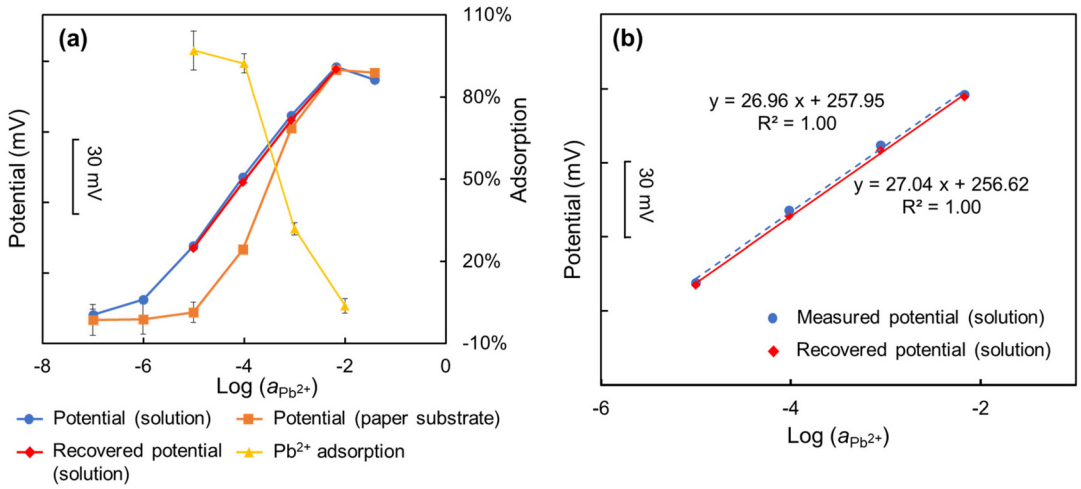

Fig. 4 Prediction of the solution-based potential readout from the measurement assisted with paper-based microfluidic solution sampling: (a) four curves are presented, namely: the adsorption of Pb^{2+} on the paper substrates; the Pb^{2+}-ISE calibration curve when electrode is utilizing paper-based solution sampling; the Pb^{2+}-ISE calibration curve in conventional solution-based measurement; and the predicted Pb^{2+}-ISE calibration curve in solution measurement obtained from measurement assisted with paper-based microfluidic solution sampling; (b) a comparison of the same Pb^{2+}-ISE between the experimental data (solution-based measurement) and the corrected potential readout from measurement assisted with paper-based microfluidic solution sampling.

solution sampling, it becomes possible to avoid calibration of the ISEs in conventional solution-based settings. Additionally, the potential readout in the measurement assisted with paper-based microfluidic solution sampling can be corrected to the Nernstian linear calibration curve, effectively addressing the issue of super-Nernstian response of ISEs coupled with paper-based solution sampling.

3.4 Corrective protocol to predict the Pb^{2+}-ISEs based potential readout in complex samples

The corrective protocol to predict the ISE's paper-based potential readout was initially established using pure solutions, where only a single salt was present ($Pb(NO_3)_2$). However, in practical analytical scenarios, the samples to be tested are often complex in ionic composition, containing multiple types of ions at different concentrations. Therefore, multiple cases were defined in this work to simulate complex testing analytical scenarios, as described in Table S1.†

In complex samples, the issue of sensor selectivity is crucial, as the introduction of interfering ions might affect the Nernstian response of the ISEs. As shown in Fig. S7, S8, S9, S10 and S11 (ESI),† the fabricated Pb^{2+}-ISEs exhibited excellent selectivity performance. This collaborates with previous reports for Pb^{2+}-ISEs with lead(II) ionophore IV.[35–37] The addition of interfering ions did not obviously affect the Nernstian response of the primary ions in most cases (Fig. S7, S8, S9 and S10†) for the recovering potentials in the range from 10^{-5} to 10^{-2} mol L^{-1}. However, it should be noted that the addition of Cd^{2+} with a high concentration (10^{-1} mol L^{-1}) affected the Nernstian response of the primary ions for the recovering potential in the low concentration range from 10^{-5} to 10^{-4} mol L^{-1} (Fig. S11†). This suggests that in most cases, Pb^{2+}-ISEs should independently be responsible for potential readout formation, unless high background electrolyte of interfering ions is present (especially important in diluted primary ion samples). The high selectivity-driven electrode response is only valid, assuming that the interfering ion has equal or higher ion adsorption affinity to the paper substrates than the primary ion. In case, the primary ion adsorption affinity to the paper substrate is much greater, the selectivity of ISEs may fail to sustain interference-free electrode response as the concentration difference between primary over interfering ions may be decreased due to competitive adsorption of the primary ion on the paper substrates. For that reason, it is important to understand the competitive adsorption of primary and interfering ions onto the paper substrates conducted in mixed ion solutions.

As shown in Fig. 5(a), unlike the selectivity of the ISEs, the adsorption of the Pb^{2+} was obviously affected by the addition of the interfering ions in most cases (2, 4, 5, and 6). However, it is worth noting that the addition of Na^+ (case 3) had almost no effect on the adsorption of Pb^{2+} on the paper substrate. For the Cd^{2+} with the same concentration of Pb^{2+}, a slight reduction in adsorption of Pb^{2+} on the paper substrate is observed at low concentrations (10^{-5} to 10^{-3} mol L^{-1}) (case 2). When the Pb^{2+} solutions ranging from 10^{-5} to 10^{-1} mol L^{-1} are mixed with a constant concentration of Cd^{2+} ions (cases 4, 5 and 6), it can be observed that the adsorption of Pb^{2+} decreases as the concentration of the interfering ion Cd^{2+} increased. This observation indicates that higher concentrations of interfering ions significantly alter the adsorption of the primary ion on the paper substrate.

To obtain the adsorption of heavy metal ions onto the paper substrates at any concentration, a multiple-segment fitting curve was employed. This curve captured the relationship between the concentration of heavy metal ions and their adsorption onto the paper substrates. The fitting process utilized multiple measured data points for each case, as listed in Table S1.† The fitting curve consisted of three sub-segments. The middle sub-segment showed a significant change in slope (concentration ranging from 10^{-4} to 10^{-2} mol L^{-1}) and was fitted using a polynomial function. The two end sub-segments (concentration ranging from 10^{-5} mol L^{-1} to 10^{-4} mol L^{-1} and from 10^{-2} mol L^{-1} to 10^{-1} mol L^{-1}) displayed smaller changes

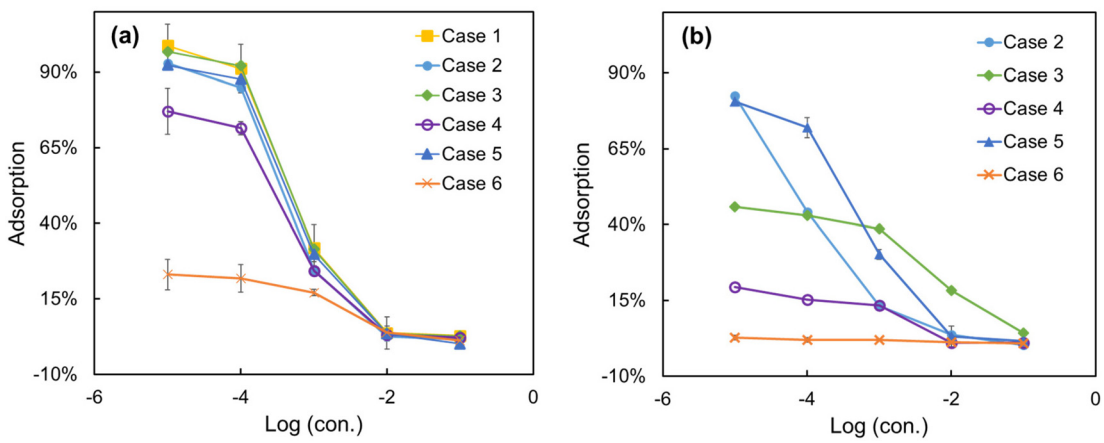

Fig. 5 Adsorption of (a) the primary ions and (b) the interfering ions on paper substrate during the potentiometric measurement with ISEs. The primary ion in cases 1–6 is Pb^{2+}; the interfering ions are Cd^{2+} or Na^+ with various concentrations (Table S1†).

in slope and were fitted using the least-squares method. The fitting of the adsorption of Pb^{2+} on the paper-based substrate in different cases can be found in Fig. S1–S6 (ESI).† For each fitting curve, two data points (non-integer concentration values) were experimentally selected and measured, indicated by red boxes. The errors between the fitted curves and the experimental results were below 2%, affirming the accuracy and validity of the fitting curves.

3.5 Corrective protocol to predict interference free sensor response for paper-based solution sampling in complex samples

In practical analytical scenarios, the sample solutions often contain multiple interfering ions, which can impact the potential response of ISEs and the adsorption of heavy metal ions on the paper substrates. These interferences affect the concentration of the target ions in the test solution and subsequently influence the potential readout related to the investigated heavy metal. This study categorized the potential background solutions of various analytical scenarios into six categories, as shown in Table S1.† The first category comprised single-ion solutions (pure solutions, interference-free solutions), while the remaining five categories represented complex situations where the test solution contained interfering ions. As shown in Fig. 6, based on the results in section 3.4 (Fig. 5), the method described in section 2.6 was used to predict interference-free sensor response for paper-based solution sampling. These results were then compared with the measured results in the standard solutions. The calculated calibration curves for the solution potential exhibited good agreement with the measured results (Fig. 6(a)). Furthermore, the slopes of the two calibration curves are nearly identical, differing by only 1.1% (Fig. 6(b)). The same method was employed for cases 3–6. The results, as shown in Fig. S12, 13, S14 and S15 (ESI),† indicated that the method described in section 2.6 can effectively recover the calibration curves obtained by paper-based solution sampling measurements to the calibration curves obtained by conventional solution-based measurements, with the calculated recovered calibration curves aligning well with the experimental results. It is worth noting that in case 6, the interfering ion, Cd^{2+} was added at a high concentration (10^{-1} mol L^{-1}), which not only significantly affected the adsorption of Pb^{2+} on the paper substrates (Fig. 5) but also interfered with the selectivity the Pb^{2+}-ISE for detecting low concentrations (lower than 10^{-5} mol L^{-1} Pb^{2+}), as shown in Fig. S11.† The adsorption of Cd^{2+} and Pb^{2+} on paper substrates involves a competitive relationship.[33] Although Pb^{2+} typically exhibits a stronger affinity for negative binding sites on the paper substrate compared to Cd^{2+}, the presence of high concentrations of Cd^{2+} ions leads to extensive occupation of these sites. This extensive occupation significantly disrupts the adsorption of Pb^{2+} on the paper substrate. This interference becomes particularly pronounced in low concentration Pb^{2+} solutions. Consequently, the solution-based potential prediction method described in section 2.6 was found unsuitable for detecting heavy metal ions with high concentrations of interfering ions and low concentrations of primary ion (case 6). However, when the concentration of the primary ion is high enough to overcome selectivity over interfering ion, the method was applicable for detecting heavy metal ions within the concentrations range of 10^{-4} mol L^{-1} to 10^{-2} mol L^{-1} (case 6). The experimental findings in measurements done in complex samples demonstrated that the method proposed is applicable to the detection of heavy metal ions in complex cases in the presence of interfering ions. The current definition of the six cases is insufficient and does not encompass all solution samples with varying matrices, particularly those containing organic compounds. Future research will focus on investigating the impact of more complex compounds on analytical results, with the objective of developing a more precise corrective model. This model will enable more accurate categorization of diverse targeted samples.

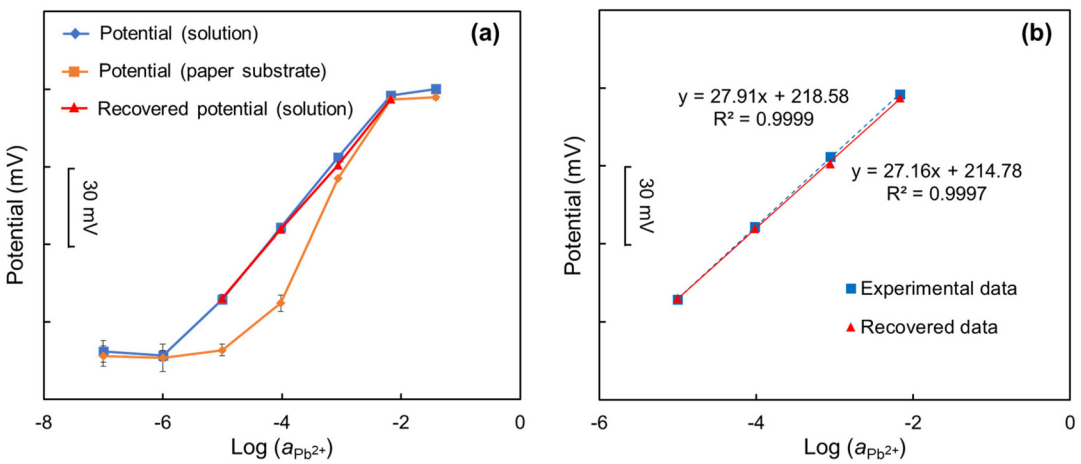

Fig. 6 Corrective protocol to predict interference free sensor response from the paper-based potential in case 2: (a) calibration curves of the fabricated Pb^{2+} ISEs on paper substrate, on standard mixed solution and recovered solution-based calibration curve from paper-based calibration curve; (b) slopes and linearities of the experimental solution-based calibration curve and the recovered solution-based calibration curve.

3.6 Determination of Pb^{2+} in complex samples

To validate the feasibility of the proposed method, three types of samples spiked with lead(II), namely lake water, laboratory recycled water, and laboratory wastewater, were tested according to the method described in section 2.7. Initially, the components of the three types of samples were analyzed using ICP-OES, Table S2 in the ESI.† Based on the measured data, it was observed that most of the interfering ions in the lake water, such as Na^+ and K^+ ions, are considered weak interferences for Pb^{2+}-ISEs. Therefore, the lake water was classified as case 3, applying the methodology of corrective prediction of interference-free potential readout of case 3. The laboratory recycled water contained low concentrations of interfering ions, such as Cd^{2+} ions, which moderately interfered with the adsorption of Pb^{2+} on the paper substrate. As a result, the laboratory recycled water was classified as case 5, applying the methodology of corrective prediction of interference-free potential readout of case 5. The laboratory wastewater, on the other hand, contained high concentrations of interfering ions, such as Cd^{2+} ions, which significantly interfered with the adsorption of Pb^{2+} on the paper substrates. Therefore, the laboratory wastewater was classified as case 6, applying the methodology of corrective prediction of interference-free potential readout of case 6. The three types of water samples are listed in Table S3.† Each sample was measured three times for both potentiometric and ICP-OES measurements and the test results are shown in Fig. 7. The results indicated that the proposed corrective protocol and the results obtained using the ICP-OES are within 10% variation. The discrepancy between potentiometric and ICP-OES measurements may be due to the use of simplified aqueous samples (cases 1–6) to approximate real samples, containing different types and concentrations of ions. This can easily lead to calculation errors, resulting in the corrective results slightly deviating from the actual. Another potential reason for the minor differences between the two methods is that the Pb^{2+}-ISE measures ionized lead(II), while the ICP-OES measures total lead. It is important to note that in this study, the potentiometric sensors measure the ion activity of heavy metal ions, and the ion concentrations were derived using empirical formulas. This approach inevitably introduced some errors, although these errors remain within an acceptable range. The direct potentiometric sensing method of the ion concentration with a self-reference pulstrode, as proposed by Xie *et al.*,[38] provides a valuable solution that enables more accurate ion concentration measurements. Overall, the proposed potentiometric measurement corrective protocol for the potential of Pb^{2+}-ISEs coupled with paper-based microfluidic sampling, which aims to predict interference-free sensor response, is a feasible method for correcting super-Nernstian response and determining lead ions in various environmental samples.

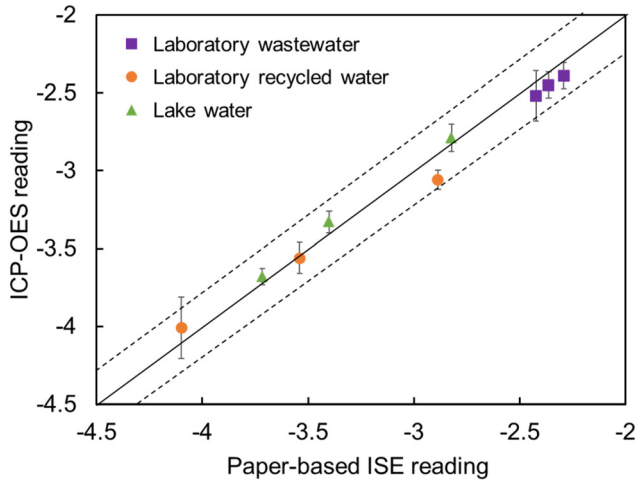

Fig. 7 Comparison of paper-based ISE and ICP-OES results in complex samples.

4 Conclusions

This study addressed the nonlinear (non-Nernstian) behavior of ISEs in potentiometric measurements assisted with paper-based microfluidic solution sampling for the detection of heavy metal ions. The investigation revealed that the adsorption of heavy metal ions onto the paper substrates is the main factor contributing to the nonlinearity of the calibration curves at low concentrations and the presence of super-Nernstian responses at intermediate concentrations. To address this issue, a corrective method to predict interference-free response of ISEs when coupled with paper-based solution sampling was developed. This was possible by quantification of the adsorption of primary ion (Pb^{2+}) or primary and interfering ion mixes (Pb^{2+} and Cd^{2+}) onto paper substrates at different concentrations. By accounting for concentration dependent adsorption of ions onto the paper substrates correction of the potential readout from conventional solution-based to assisted paper-based solution sampling (or *vice versa*) was possible. This novel approach successfully quantified the underlying cause of the nonlinear behavior (non-Nernstian) of calibration curves in ISEs measurement assisted with paper-based solution sampling during the detection of heavy metal ions.

Furthermore, the ion selectivity of the ISEs was evaluated, and the adsorption of heavy metal ions in a competitive environment of primary and interfering ions was investigated. The findings demonstrated that the accurate adsorption of heavy metal ions onto paper substrates, in combination with the proposed theoretical corrective prediction of interference-free potential readout, is also applicable for detecting heavy metal ions in complex analytical scenarios. It was further validated in lead(II) samples with real background, namely lake water, laboratory recycled water, and laboratory wastewater. The results obtained from corrective prediction of interference-free potential readout and ICP-OES exhibited good agreement with less than 10% error.

In summary, the results advanced the understanding of the cause of non-Nernstian behavior of ISEs when assisted with paper-based solution sampling. This allowed the development

of the method where the paper substrate does not have to be modified to eliminate the non-Nernstian behavior of the sensor, but instead through adsorption, the interference-free response of the sensor can be obtained. This simplifies the measuring set-up design and allows for more cost-effective *in situ* detection of heavy metal ions with paper-based solution sampling.

Author contributions

Mingpeng Yang: methodology, investigation, formal analysis, and writing – original draft; Rochelle Silva: methodology and investigation; Ke Zhao: methodology and investigation; Ruiyu Ding: methodology and investigation; Jit Loong Cyrus Foo: methodology and investigation; Liya Ge: investigation, review & editing; and Grzegorz Lisak: conceptualization, methodology, resources, writing – review & editing, supervision, funding acquisition, and project administration.

Data availability

Data will be made available on request.

Conflicts of interest

There are no conflicts to declare.

Acknowledgements

This research was supported by the National Research Foundation, Singapore, and PUB, Singapore's National Water Agency, under its RIE2025 Urban Solutions and Sustainability (USS) (Water) Centre of Excellence (CoE) Programme, which provides funding to the Nanyang Environment & Water Research Institute (NEWRI) of the Nanyang Technological University (NTU, Singapore). Any opinions, findings, conclusions or recommendations expressed in this material are those of the author(s) and do not reflect the views of the National Research Foundation, Singapore, and PUB, Singapore's National Water Agency.

References

1 S. Mitra, A. J. Chakraborty, A. M. Tareq, T. B. Emran, F. Nainu, A. Khusro, A. M. Idris, M. U. Khandaker, H. Osman and F. A. Alhumaydhi, *J. King Saud Univ., Sci.*, 2022, 101865.
2 N. Munir, M. Jahangeer, A. Bouyahya, N. El Omari, R. Ghchime, A. Balahbib, S. Aboulaghras, Z. Mahmood, M. Akram and S. M. Ali Shah, *Sustainability*, 2022, **14**, 161.
3 Z. Wang, P. Luo, X. Zha, C. Xu, S. Kang, M. Zhou, D. Nover and Y. Wang, *J. Cleaner Prod.*, 2022, 134043.
4 Y. Liu, J. Zhao, K. Zhao, S. Zhang, R. Tian, M. Chang, Y. Wang, X. Li, L. Ge and G. Lisak, *J. Environ. Chem. Eng.*, 2023, **11**, 111563.
5 Y. Pan, X. Liu, L. Qian, Y. Cui, X. Zheng, Y. Kang, X. Fu, S. Wang, P. Wang and D. Wang, *Sens. Actuators, B*, 2022, **352**, 130971.
6 H. Sharifi, J. Tashkhourian and B. Hemmateenejad, *Sens. Actuators, B*, 2022, **359**, 131551.
7 Q. Ding, C. Li, H. Wang, C. Xu and H. Kuang, *Chem. Commun.*, 2021, **57**, 7215–7231.
8 G. Lisak, *Environ. Pollut.*, 2021, **289**, 117882.
9 J. Ding and W. Qin, *TrAC, Trends Anal. Chem.*, 2020, **124**, 115803.
10 M.-R. Huang and X.-G. Li, *Prog. Mater. Sci.*, 2022, **125**, 100885.
11 M. Yang, N. Sun, Y. Luo, X. Lai, P. Li and Z. Zhang, *Biomicrofluidics*, 2022, **16**, 031503.
12 X. Lai, M. Yang, H. Wu and D. Li, *Micromachines*, 2022, **13**, 1363.
13 R. Pol, F. Céspedes, D. Gabriel and M. Baeza, *Sens. Actuators, B*, 2019, **290**, 364–370.
14 C.-C. Tseng, S.-Y. Lu, S.-J. Chen, J.-M. Wang, L.-M. Fu and Y.-H. Wu, *Anal. Chim. Acta*, 2022, **1203**, 339722.
15 J. Gallardo-Gonzalez, A. Baraket, S. Boudjaoui, T. Metzner, F. Hauser, T. Rößler, S. Krause, N. Zine, A. Streklas and A. Alcácer, *Sci. Total Environ.*, 2019, **653**, 1223–1230.
16 M. Yang, N. Sun, X. Lai, J. Wu, L. Wu, X. Zhao and L. Feng, *ACS Sens.*, 2023, **8**, 176–186.
17 R. Ding, Y. H. Cheong, A. Ahamed and G. Lisak, *Anal. Chem.*, 2021, **93**(4), 1880–1888.
18 V. Krikstolaityte, R. Ding, E. C. H. Xia and G. Lisak, *TrAC, Trends Anal. Chem.*, 2020, **133**, 116070.
19 R. Ding, M. Fiedoruk-Pogrebniak, M. Pokrzywnicka, R. Koncki, J. Bobacka and G. Lisak, *Sens. Actuators, B*, 2020, **323**, 128680.
20 R. Silva, K. Zhao, R. Ding, W. P. Chan, M. Yang, J. S. Q. Yip and G. Lisak, *Analyst*, 2022, **147**, 4500–4509.
21 R. Silva, A. Ahamed, Y. H. Cheong, K. Zhao, R. Ding and G. Lisak, *Anal. Chim. Acta*, 2022, **1197**, 339495.
22 R. Ding, V. Krikstolaityte and G. Lisak, *Sens. Actuators, B*, 2019, **290**, 347–356.
23 R. Ding, Y. H. Cheong, K. Zhao and G. Lisak, *Sens. Actuators, B*, 2021, **347**, 130567.
24 J. Bobacka, *Anal. Chem.*, 1999, **71**, 4932–4937.
25 V. Gupta, R. Mangla and S. Agarwal, *Electroanalysis*, 2002, **14**, 1127–1132.
26 A. Ceresa and E. Pretsch, *Anal. Chim. Acta*, 1999, **395**, 41–52.
27 E. Malinowska, Z. Brzózka, K. Kasiura, R. J. Egberink and D. N. Reinhoudt, *Anal. Chim. Acta*, 1994, **298**, 253–258.
28 T. J. Wolery, *Geochemistry*, Springer, 1998, pp. 124–126.
29 H. S. Harned, B. B. Owen and C. King, *J. Electrochem. Soc.*, 1959, **106**, 15C.
30 J. Kielland, *J. Am. Chem. Soc.*, 1937, **59**, 1675–1678.
31 J. Gou, W. Zhang, X.-F. Wang, D. Hao, H. Shen, N. You and W.-Y. Long, *Chemosphere*, 2023, **339**, 139705.

32 T. Satarpai, J. Shiowatana and A. Siripinyanond, *Talanta*, 2016, **154**, 504–510.
33 L. Lv, M. P. Hor, F. Su and X. Zhao, *J. Colloid Interface Sci.*, 2005, **287**, 178–184.
34 R. Ding, N. K. Joon, A. Ahamed, A. Shafaat, M. Guzinski, M. Wagner, T. Ruzgas, J. Bobacka and G. Lisak, *Sens. Actuators, B*, 2021, **344**, 130200.
35 M. Guziński, G. Lisak, J. Kupis, A. Jasiński and M. Bocheńska, *Anal. Chim. Acta*, 2013, **791**, 1–12.
36 X.-G. Li, X.-L. Ma and M.-R. Huang, *Talanta*, 2009, **78**, 498–505.
37 M. Guziński, G. Lisak, T. Sokalski, J. Bobacka, A. Ivaska, M. Bocheńska and A. Lewenstam, *Anal. Chem.*, 2013, **85**, 1555–1561.
38 W. Gao, X. Xie and E. Bakker, *ACS Sens.*, 2020, **5**, 313–318.